Journal of Ship Production and Design, Vol. 26, No. 3, August 2010, pp. 219–230

Resistance of a Compartmented Surface-Effect Ship

Alexander H. Day,* **David Clelland,*** **Lawrence J. Doctors,**† and **Philip Beveridge***

* *Department of Naval Architecture and Marine Engineering, The University of Strathclyde, Glasgow, Scotland*
† *School of Mechanical and Manufacturing Engineering, The University of New South Wales, Sydney, NSW, Australia*

A series of carefully controlled experiments on the resistance of a model of a compartmented surface-effect ship has been conducted in a towing tank. Configurations of the model included cases encompassing one subcushion and two subcushions, as well as differing values of the pressures in the subcushions. It was shown that a reduced total resistance in the appropriate range of Froude number could be achieved in this manner. Furthermore, the previously developed theory for the resistance of a surface-effect ship was verified for the model for a Froude number greater than 0.40.

Keywords: surface effect ships; resistance (general)

1. Introduction

1.1. Background

One is necessarily interested in minimizing the resistance of a ship during the design process, in order to reduce the engine capacity and, consequently, fuel consumption, operational cost, and subsequent environmental damage.

With the advent of computers, this minimization process became feasible, because it was then possible to compute rapidly the wave resistance based on the method of, say, Michell (1898). This procedure could be placed within software designed to modify the hull shape until the desired minimum was achieved. Of course, the total resistance in such a method also accounts for the frictional resistance, but it was generally assumed that this component of friction varied little with the hull shape.

The earliest paper to apply this approach was that of Lin et al (1963). Other, later, research that adopted this approach includes the work published by Doctors and Day (1995, 1997). These last two papers used the genetic algorithm (GA) for the optimization process. The GA has the advantage of being an efficient optimizer that can easily account for strongly nonlinear effects in the analysis. These nonlinear effects would be constraints on the geometric smoothness of the hull, as well as other nonhydrodynamic requirements.

An obvious difficulty with determining optimal hullforms is that the resultant shape will be optimal for one speed only. Thus, one is likely to design a hullform that is a compromise for a range of speeds. This is because it is not practical to change a rigid hull as the speed varies.

On the other hand, the possibility of changing the effective hullform exists for the air-cushion vehicle (ACV) and for the surface-effect ship (SES), because it is practical to alter the cushion pressure in different areas, on the basis that the cushion is divided into subcushions.

This idea was pursued by Doctors (1997), who applied the method of Lagrange Multipliers. This optimization technique is purely linear, but permits the inclusions of simple constraints—such as the need to fix the desired total displacement of the vessel. Thus, a consequent deficiency is the possibility of generating mathematically possible, but impractical, solutions for the pressures in the subcushions, which may be negative over part of the speed range. Despite this, the Lagrange-Multiplier method could generate practical pressure distributions for useful parts of the speed range that led to a vastly reduced wave resistance. The GA was also applied by Tuck and Lazauskas (2001), who were able to confirm the work of Doctors and also to create even more useful pressure distributions.

A difficulty with employing multiple subcushions with an ACV is the need to design skirts or seals to support the pressure differentials between the subcushions. A good way to eliminate part of the complication of seals is to apply the idea of subcushions to the SES. This was done, for example, by Doctors et al. (2005). In fact, it is feasible to create a two-subcushion vessel by adding just one additional transverse seal. Numerical experiments in that paper indicated that a suitable location for this seal was about one-third of the distance aft of the bow of the vessel.

Manuscript received by JSPD Committee November 2009; accepted May 2010.

For this location of the seal, the optimal pressure distribution generally involves higher pressure in the aft subcushion than in the forward subcushion. The practical benefit of this configuration is that this pressure differential can be sustained by a finger seal, similar to that employed at the bow of the vessel. This seal is regarded as suffering a smaller additional resistance component (seal drag) than the lobe seal generally used at the stern of the vessel; additionally, unlike the lobe seal, it does not require any additional machinery or ducting for inflation.

We should emphasize that linear theory states that the optimal pressure-hull distribution must possess fore-and-aft symmetry. Hence, one could achieve a greater reduction in resistance by using two additional transverse seals (thus creating three subcushions). It is debatable whether the advantages of a three-subcushion configuration would justify the additional seal.

This is especially true, as the aftermost of the two internal seals in an optimal three-subcushion SES would have to sustain a higher pressure on the forward side than on the aft side, requiring a lobe-type seal. Given that the marginal gain in resistance between two and three subcushions is likely to be smaller than that between one and two subcushions, even before seal drag is factored into the equation, then the additional drag and mechanical complexity of a second lobe seal is unlikely to be justified.

1.2. Current work

In the present research, we shall concentrate our efforts on the two-subcushion SES, because this vessel concept is the simplest one that offers a good reduction in both wave resistance and total resistance.

Practical work on this concept has already been presented by Steen and Adriaenssens (2005). The authors used a hinged-plate divider to support the pressure differential between the aft and the forward subcushions, rather than a conventional finger seal. This is unfortunate, because a hinged plate (particularly one at a large angle of attack of around 45 deg), suffers a very high drag. So, it is unlikely that any reduction in total resistance could be achieved in this way. In addition, the correlation between the measured and the theoretical total resistance was poor (up to a 40% underprediction) for a substantial part of the speed range. This was due to the unrealistic assumptions in their theory.

In the first stage of the study described here, Beveridge (2009) essentially replicated the work of Steen and Adriaenssens (2005) in that he also tested a split-cushion SES model. Beveridge intentionally employed thin sidehulls, so that the wave-interference effects would be maximized. A diagram of his experiment appears in Fig. 1*a*. This shows the main features defining the problem.

A sketch of the model itself appears in Fig. 1*b*, where the principal components are noted. The model incorporates three fans to supply, respectively, the aft-lobe seal, the aft subcushion, and the bow subcushion.

In order to largely eliminate the undesired excessive drag of the intersubcushion seal drag, he used a finger seal. This possesses much less drag than a fixed planing plate. Furthermore, Beveridge incorporated a novel adjustable subwetdeck that this additional seal was attached to. He was therefore able to move the seal vertically, during a run in the towing tank. In this manner, the hydrodynamically deflected lower part of the fingers could be maintained at a minimum and the total drag of the vessel would be reduced even further. He was able to adjust the height of this

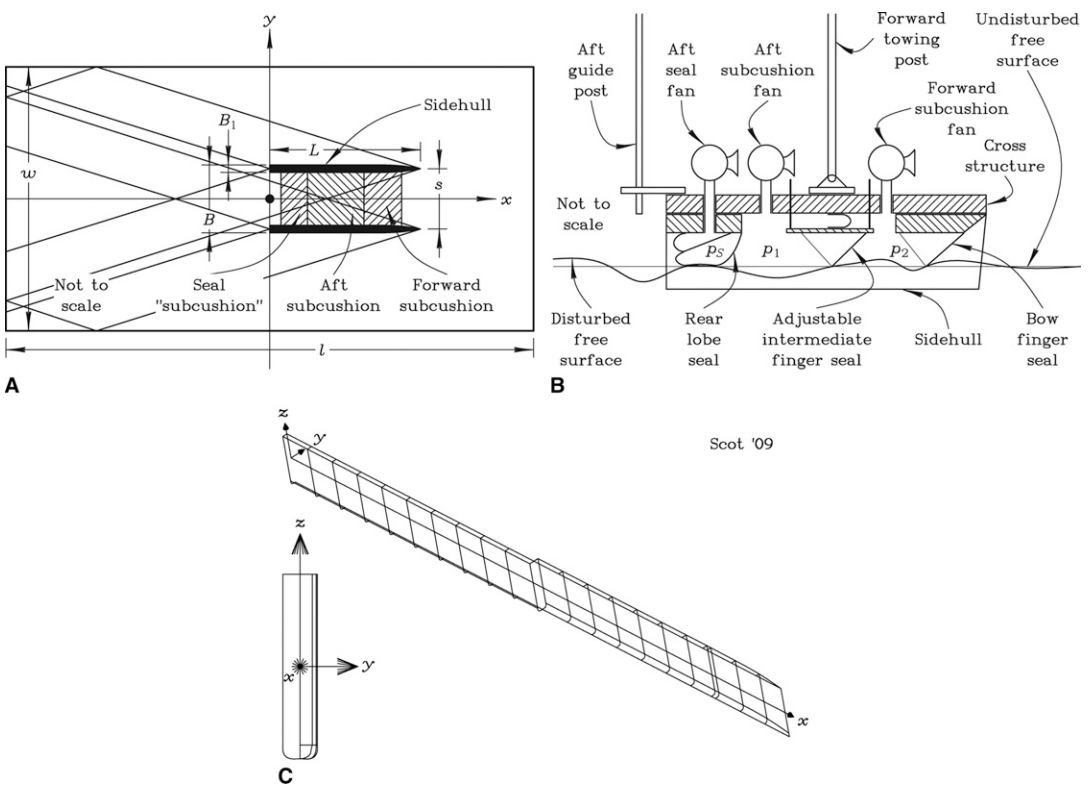

Fig. 1 Problem definition. *a* Plan view of towing tank. *b* Profile view of model. *c* Pictorial view of model SES sidehull

seal in an effective manner by the aid of a videocamera that was positioned within the aft subcushion.

A pictorial view of Beveridge's sidehull is shown in Fig. 1*c*. It should be noted that a split view is shown. That is, only the port bow and the starboard stern. This explains the apparently laterally asymmetric nature of the body plan in the lower left-hand corner of this figure.

It is pleasing to record that Beveridge was able to demonstrate a substantial reduction in the drag of his SES model because of the care in the design, construction, and testing of the model.

2. Theory

A characteristic of an SES is that the sidehulls are relatively thin compared with their length. Similarly, the cushion depression is also small compared with the cushion length. Thus, one can legitimately use linearized free-surface water-wave theory for computing the wave resistance.

Newman and Poole (1962) and Barratt (1965) provided two early examples of application of the linearized theory to pure pressure distributions, representing an ACV. Newman and Poole's calculations included the interesting effects of finite canal width and finite water depth, thus simulating problematic features of a practical experiment in a towing tank or real operational difficulties, such as driving an ACV in shallow water. This work is based on some earlier research by Sretensky (1936).

The inclusion of sidehulls to complete the idealized modeling of an SES was described in detail by Doctors (1993) and Doctors and McKesson (2006). In this approach, the contributions to the wave disturbances are mathematically equivalent to source distributions alone. That is, lateral velocities induced on a sidehull by the cushion and the other sidehull are ignored where, strictly speaking, a vorticity distribution should be distributed on the centerplane of the sidehulls in order to complete the mathematical model. Similar arguments apply to the idealized need to account for the asymmetric demihulls often employed in SES designs.

The inclusion of such vorticity distributions adds considerably to the computational complexity of the computer software. It can be shown, nevertheless, that the resulting corrections are likely to be small. To date, no person has implemented this more sophisticated technique in its entirety.

The sidehulls of a typical SES possess transom sterns. Thus, one is also required to model the flow past the transoms in a realistic manner.

Oving (1985) conducted some early research into the unwetting of transoms of differing beam-to-draft ratios. Doctors and Day (1997) created their "firehose" analogue for estimating the extent and shape of the hollow created behind the stern. They achieved creditable correlation for predictions of total resistance with a number of towing-tank experiments on models of high-speed catamarans of that era.

This work has since been enhanced in a number of ways, culminating in the papers by Doctors (2007) and Doctors et al. (2007). This final effort resulted in two simple algebraic formulas. The formulas were essentially regression fits to experimental data obtained for a large number of transom-area aspect ratios and Froude numbers. The first formula gives an estimate of the length of the hollow, for use in the wave-resistance calculation, which is to be applied to a virtual hull consisting of the physical hull together with the hollow behind the transom. The second formula is used to estimate the unwetting or ventilation of the transom, thus providing a prediction of the transom drag (or hydrostatic drag) of the vessel.

With regard to the seal drag, the two methods of Doctors and McKesson (2006) were used. The method for the bow seal was based on assuming that the fingers deflect and behave like planing surfaces. Thus, both profile and frictional drag are predicted. Currently, the method for the stern lobe seal considers just the frictional drag.

These theories were applied to the measured conditions in the experiment. That is, the time-averaged measured subcushion pressures were used in the calculations of the wave resistance.

The physical properties of the water and air, as well as the dimensions of the towing tank are listed in Table 1. These data were used in the numerical computations for the analysis of the experiments.

3. Physical equipment

3.1. Model design and construction

The model was designed and constructed specifically for this test program, with the intention of reflecting most aspects of typical current SES designs. The model was designed to be semicaptive (free to sink, trim and heel, and constrained in surge, sway, and yaw) and to give adequate scope for longitudinal-center-of-gravity (LCG) movements to allow investigation of the partitioned cushion. This required a very lightweight model, especially given the weight of equipment and instrumentation that the model was required to carry.

In order to allow the desired range of Froude numbers to be investigated in the Kelvin Hydrodynamic Laboratory towing tank, the nominal model length was chosen to be 2.0 m; the nominal length-to-beam-ratio was chosen as 3.5 based on typical current practice. The target ratio of cushion displacement to hydrostatic displacement was 2.45, and the target ratio of draft to cushion depression was 4.0. It was decided to design the sidehulls to be symmetrical about their own centerplane. This leads to a shorter cushion with respect to hull length, compared with many working SES designs, since the bow seal is located in the parallel body in order to ensure efficient operation.

Table 1 Data pertaining to the computations

Item	Symbol	Value
Overall beam (m)	B	0.570
Acceleration due to gravity (m/s^2)	g	9.8067
Density of water (kg/m^3)	ρ	998.3
Windage area (m^2)	A_{ref}	0.1419
Density of air (kg/m^3)	ρ_{a}	1.225
Aerodynamic drag coefficient	C_{D}	0.800
Friction line	C_{F}	ITTC 1957
Frictional form factor	f_{F}	1.150
Longitudinal smoothing factor (m^{-1})	α_x	10.0
Transverse smoothing factor (m^{-1})	α_y	10.0
Run length of towing tank (m)	l	64.0
Width of towing tank (m)	w	4.572
Depth of towing tank (m)	d	2.005

After some iteration, the final design was developed as shown in Fig. 1*b*; principal dimensions are summarized in Tables 2 and 3.

The main hulls were machined from Divinycell foam, reinforced with plywood layer at the upper surface, and finished with an epoxy fairing paste. The main crossdeck structure was manufactured from a sandwich construction of Divinycell and thin plywood in order to achieve high stiffness at low weight.

The model was designed to be run in three configurations: firstly as a conventional single-cushion SES, secondly, as a partitioned-cushion SES, with the aft subcushion at a higher pressure than the forward subcushion, and finally as a short-cushion SES. This required the use of a total of three seals.

A conventional finger seal was used in the bow, with eight fingers; the slope of the leading edge of each finger was 45 deg to the vertical. Particular attention was paid to ensuring that the lower edge of each finger lay on a horizontal plane with the vessel in level trim. The fingers were constructed from thin flexible plastic sheet, mounted on a thin plywood sheet in order to allow the seal to be removed as a unit. The stern seal was designed as a two-lobe seal; the open ends sealed onto the inner hull surface to minimize friction between the seal and the hull and to allow the seal to take up the most appropriate configuration under way.

Table 2 Data for sidehull of SES model

Item	Symbol	Value
Displacement mass (kg)	Δ	4.533
Waterline length (m)	L	2.005
Waterline beam (m)	B_1	0.030
Nominal draft (m)	T	0.080
Waterplane-area coefficient	C_{WP}	0.9561
Maximum section coefficient	C_M	0.9842
Block coefficient	C_B	0.9403
Prismatic coefficient	C_P	0.9555
Slenderness coefficient	$L/\nabla^{1/3}$	12.15

Table 3 Data for subcushions of SES model

Item	Symbol	Value
Transom coordinate (m)	x_t	0.000
Rear-seal start station (m)	x_0	0.095
Aft-subcushion start station (m)	x_1	0.245
Fwd-subcushion start station (m)	x_2	1.170
Fwd-subcushion stop station (m)	x_3	1.752
Cushion beam (m)	B_C	0.510

The inner seal was also of the finger type and was designed to be identical to the bow seal, on the assumption that when the model ran as a partitioned cushion, the pressure would always be higher in the aft subcushion than in the forward subcushion. However, because the water level in the cushion varies with speed, this seal had to be constructed to be movable. The plywood base of the seal was attached to three aluminum rods, running in low-friction bushes. Each rod was moved by a miniature ball-screw actuator, with a stroke of 100 mm. These were equipped with microcontrollers allowing an analogue voltage to set the target position. Careful setup ensured that the orientation of the seal relative to the hull remained constant when the three actuators moved.

The upper part of the base was sealed to the hull using a transverse bellows-like flexible seal. The stroke of the actuators was sufficient to allow the inner seal to be lifted clear of the water for cases in which the model was run as a conventional SES. This is illustrated in Fig. 1*b*.

Cushion pressure was generated using lightweight 12 V fans, one forward of the inner seal and one aft of the seal. A third fan was used to pressurize the rear seal. It was found that with the fans blowing, a visible depression was created in the free surface, so a simple diffuser was fitted to the duct exit for each of the lift fans. The fans were run in open-loop control, with fan speed proportional to supply voltage. This voltage was controlled manually, using the digital readout of the high-current power supplies used to drive the fans. The power supplies could be set to the desired level then switched on and off without further adjustment.

A photograph from the stern of the model is presented in Fig. 2*a*. This shows the two-lobe rear seal as well as the central divider finger seal and the bow-finger seal. A view of the model underway during a typical run in the towing tank is seen in Fig. 2*b*.

3.2. Instrumentation and model setup

The towing point of the model was located at midships on the cross deck structure. Following the standard ITTC procedure (section 7.5-2-02-01) the model was attached to the tow post using a connection that only transmits a horizontal tow force. Towing force was measured using a high-quality off-the-shelf tension/compression load cell. The model was thus free to sink, trim, and heel; freedom in heel prevents any torsional moments from affecting the load cell. The model was restrained in yaw using a

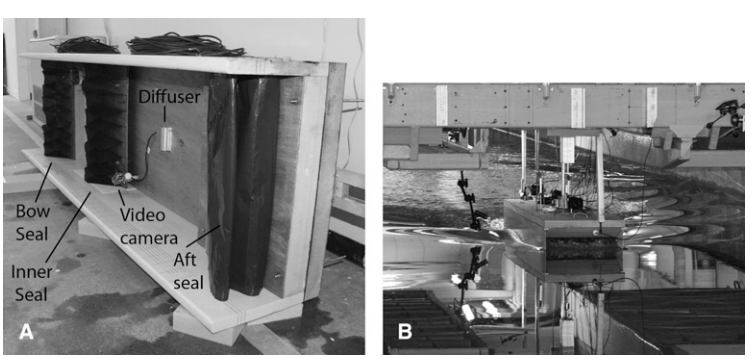

Fig. 2 Towing-tank experiments. *a* View of stern. *b* Model undergoing a test

conventional arrangement of a vertically mounted circular post located between two horizontally mounted rollers. The model was carefully ballasted to ensure level heel at zero speed in the on-cushion condition; however, the freedom in heel did prevent the completion of the test series planned at the highest displacement of 40.4 kg due to loss of transverse stability at speed, as described in section 4.3.

It should be pointed out that it would be ideal to tow the model from a point corresponding to the vertical location thrust line. However, in the current case, the model does not represent a real ship design, and thus the thrust line is unknown. The extremely slim hulls would in any case preclude this. Towing the model from the deck level induces trim by the bow. This was not corrected—for two reasons. Firstly, the trim was found to be small in practice. Secondly, since the main goal of the experimental study was to explore the comparative performance of different cushion arrangements, it was felt that the impact of bow-down trim would affect different arrangements in a similar manner and thus would not affect the conclusions regarding relative performance.

In addition to the towing force, the model attitude longitudinally was determined from measurement of vertical position using an LVDT, and measurement of trim employed an electronic inclinometer. It was found to be important to use a gravity-referenced device to measure the trim in this case. If trim were calculated from two measurements of vertical position, the trim would naturally be referenced to the off-cushion case. The model does not necessarily float in level trim off-cushion, and because of the presence of the complicated submerged geometry off-cushion (with in-cushion videocameras possibly submerged, for example), it is not easy to calculate the trim in this condition. In practice, there are two values that are of interest, first the value with the vessel on-cushion but at zero speed and second with the vessel underway. Both of these can be determined unambiguously in absolute terms using an inclinometer.

Air pressure was measured in both subcushions and in the rear seal using differential-pressure transducers mounted on the deck. It was found desirable to provide a small vent hole in the tube running through the deck to the pressure transducer, in order to allow the pressure in the tube to return to atmospheric between tests, even when the exit of the tube was submerged. This occurred in the higher load cases with LCG aft. In cases using a partitioned cushion, the voltage signal to the inner seal was logged in order to establish when the seal vertical position had been stabilized and to identify the steady-state portion of the run. The voltage from the power supply driving each fan was also logged.

Finally, a total of five videocameras were used; three waterproof cameras were mounted in the model, two in the forward subcushion and one in the aft subcushion in order to observe the flow around the seals, while two were mounted on the carriage to examine flow externally.

4. Execution of experiments

4.1. Test procedure

The model was tested in Strathclyde University's Kelvin Hydrodynamic Laboratory. The nominal tank dimensions are 76.2 by 4.6 by 2.5 m. Tests were run with water depth of 2.005 m, in order to give adequate clearance for the equipment mounted on the model deck under the towing post. The first stage of the test program, described by Beveridge (2009), took place in April 2009; the model was subsequently developed further on the basis of this experience, and the main set of tests was carried out in June 2009.

The procedure for these tests is slightly more complicated than for conventional displacement ship tests. Initial zeroes were taken with all fans off and the model off-cushion. In cases for which the cushion was to be partitioned, the inner seal was lowered to its full extent. The rear seal was then pressurized, and then the air cushion(s). It was found that the ride height was strongly influenced by rear seal pressure. It was found that the rear seal could find a stable equilibrium in either of two positions; in one case, the seal could invert and face forward. This could easily be observed on the videocamera. In such cases, the seal was then adjusted manually to face aft. A second set of zeroes was then taken in order to establish the zero-speed on-cushion attitude before the carriage moved off.

For partitioned cushion cases, once the model had reached steady speed, the inner seal was adjusted manually, using a potentiometer, to reduce the associated resistance. This was guided by views of the seal from the in-cushion videocameras. This operation required care and some practice; it was found that if the seal were raised too far, then the pressure equalized throughout the cushion, and the pressure differential between the forward and aft subcushions could not easily be reestablished in the available time of the run.

4.2. Uncertainty analysis

For previous conventional displacement ship tests, a formal uncertainty analysis has indicated a level of uncertainty in the measured resistance of around 0.6% using the equipment employed here. The bias error was found to be typically around 0.5%. This systematic error is related to equipment performance and model installation and, as such, is likely to remain approximately consistent with these results, because the equipment used and procedures adopted are very similar. However, it is likely that the uncertainty related to precision is somewhat higher during these tests, compared with tests of a displacement ship, as there are a number of additional sources of uncertainty, some of which are extremely difficult to quantify.

As described previously, the model carries a lot of equipment, and consequently there is a greater than usual number of cables running between the carriage and the model. This contributes additional uncertainty to the weight of the model, because it is difficult to determine how much of the weight of the cables is carried by the model, and how much by the carriage; considerable effort was expended in trying to ensure that the cables hung during weighing as they were observed to do during testing.

A further source of uncertainty in the weight of the vessel is related to the possibility of small amounts of water being trapped in a variety of locations that were submerged off-cushion; these included the space above the inner seal and inside the open-ended rear seal. The presence of substantial quantities of water in the rear seal could clearly be observed on the videocamera and, over the course of the test campaign, a few runs were terminated as a result of this phenomenon. However, the presence of a small quantity of water inside the seal might not have been detected.

It was also found that the pressure in the air cushions varied slightly from test to test, even though the fan voltage was highly repeatable. In the context of these semicaptive tests, this has the effect of redistributing displacement from the cushion to the hulls or vice versa. Finally, during the tests involving the partitioned cushion, the involvement of a human operator moving the seal based on visual observation inevitably leads to some additional uncertainty in the drag caused by the inner seal.

Nonetheless, when a series of repeat tests over a wide range of speeds and loading conditions was carried out, it was found that the points generally lay within around ±0.5% with the single cushion and with the shorter single cushion. The only exception to this occurred in the light-displacement tests at the point in which the bow wave could interact with the rear seal. In this case, the repeatability was slightly poorer. As soon as the wave passed under the seal, the repeatability returned to its previous level.

With the partitioned cushion case, subtle differences in setup from test to test resulted in variations of the ratio of the pressure between aft and forward subcushions. This would also lead to somewhat poorer repeatability.

4.3. Observations on experiments

The test campaign was split into two main parts. In the first part, the resistance of the single-cushion SES was studied with varying displacement. In the second part, the effect of varying the cushion configuration was studied while holding the displacement constant. In each case, a series of small additional studies was carried out in order to explore sensitivity of the results to factors other than speed or displacement.

The single-cushion tests were carried out at three displacements. A higher displacement was attempted, but the model lost stability underway and developed a large angle of loll, so the highest displacement was not pursued.

The results showed the expected behavior, with a pronounced hump occurring at a speed of around 1.6 m/s (corresponding to a Froude number based on cushion length of 0.36), followed by a rapid drop in total resistance. As would be expected, the resistance increased with displacement.

A number of interesting observations was made during the experimental test program. In particular, it could be seen that there was a sharp drop in the resistance for the single-cushion configuration with a displacement of 28.4 kg around a speed of 1.55 m/s (Froude number of 0.35). This phenomenon was found to be repeatable. After close observations of the videotapes of a large number of runs around this speed region, it was observed that there was a strong interaction between the wave system generated from the bow of each sidehull and the rear seal. The bow waves interact to form a wave on the centerplane of the vessel resembling a "rooster tail." As speed is increased, this wave appears to move aft, and at the point of highest resistance, this wave sits on the forward surface of the rear seal, causing a visible distortion of the seal transversely, and raising the water level on the forward surface of the seal. If the speed is then increased slightly, the wave emerges from underneath the seal. Consequently, the seal resumes its more normal shape, and the resistance drops sharply. This was found to happen in a very well defined and narrow speed range; this effect disappears in the heavier displacement cases.

The tests on variable configuration were carried out at the intermediate displacement. This was chosen as being near to the initial design condition, while giving enough movable ballast to accommodate a range of LCG conditions corresponding to the different cushion conditions. The baseline case was the single full-length cushion. The two other configurations of interest were the partitioned cushion, with the aft subcushion pressure higher than that forward, and the aft subcushion only. This last condition was achieved by completely removing the front seal.

The main practical problem faced in the partitioned-cushion cases was the control of the pressure ratio between the aft and forward subcushions. This was found to depend on many parameters; the fan speed obviously had an effect, but leakage from the aft cushion into the forward cushion under the inner seal was also a factor. This in turn depended on inner seal height, speed, and trim. In some cases, the forward fan was switched off completely, and the desired forward cushion pressure achieved purely from leakage. The maximum variation in subcushion pressure ratio (forward-subcushion pressure to aft-subcushion pressure) was approximately 20% from the mean value of about 0.47. Points obtained outside this range were not included in the plots.

5. Measured subcushion pressures

5.1. Summary of test series

Six series of tests on the model SES were completed. These tests are summarized in Table 4.

Series 1, series 2, and series 3 were three identical single-cushion configurations, with the only parameter differentiating them being the displacement Δ. The three displacements were, respectively, 28.4, 32.4, and 36.4 kg. The single-cushion configuration was achieved by removing the additional transverse seal.

The purpose of these three series was to examine the validity of linearity, already referred to previously. Had the model been a

Table 4 Particulars of tests

Series	Configuration	Displacement Δ (kg)	Center of gravity LCG (m)	Nominal pressure ratio p_2/p_1	No. of runs
1	Single large	28.4	0.927	1	39
2	Single large	32.4	0.914	1	24
3	Single large	36.4	0.910	1	21
4	Single large	40.4	0.920	1	1
5	Partition full	32.4	0.814	0.5	33
6	Single short	32.4	0.747	0	33

pure ACV, the total resistance (essentially, the wave resistance) would ideally be proportional to the square of the cushion pressure (and, hence, the weight of the model). In our case, the situation is rather more complicated, because there are additional and significant components of resistance. Consequently, the total resistance is expected to be a different function of the weight. Despite this, it is possible to at least test the relative accuracy of the theory for the three different levels of cushion pressure.

Series 4 was also a single-cushion configuration, and it consisted of just one point at a displacement of 40.4 kg. Using the first three series, this permitted us to plot a curve of resistance (both theory and experiment), at the selected Froude number of 0.32, as a function of displacement, with a total of four points.

Next, series 5 was the first two-subcushion case tested. It was done with a displacement of 32.4 kg, as in series 2. The aim of this series was to compare the resistance behavior of the model, with the anticipation that an improvement could be achieved.

Finally, series 6 was physically a single-subcushion configuration. In the experiment, this was achieved by removing the bow-transverse seal. However, we viewed this as a second version of a two-subcushion configuration, with a zero pressure in the forward subcushion. Thus, we could argue that series 2, series 5, and series 6 were effectively three versions of a two-subcushion configuration, possessing the same total displacement of 32.4 kg, but differing with respect to the subcushion pressure ratio.

5.2. Temporal pressure traces

A selection of four temporal pressure traces is now presented in the four parts of Fig. 3.

Figure 3*a* is an example from series 1 for the single-subcushion configuration. The first curve is a plot of the carriage speed U, illustrating the essentially constant acceleration during the first phase of the carriage motion. This is followed by the usual constant-speed phase. The staircase nature of the constant-acceleration curve is an artifice of the data-logging system; in fact, the true curve is a very close approximation to a straight line.

The stern-seal pressure p_S, the aft-subcushion pressure p_1, and the forward-subcushion pressure p_2 all exhibit an oscillatory feature. The pressures have been rendered dimensionless using the water density ρ, the acceleration due to gravity g, and the model length L. The pressures are plotted as a function of the dimensionless time $t\sqrt{g/L}$, in which t is the time.

Only a few of the runs in the towing tank had this oscillatory characteristic. It is thought that this might relate to an interaction between the cushion-air-feed system, the seals, and the hydrodynamics of the water. This does not constitute a problem for the analysis, because the long-term behavior of the curves is a smooth one.

We emphasize here that these oscillations *are not related to the unsteady starting phenomena*, first discussed in detail by Wehausen (1964) and studied experimentally by Day et al. (2009). Our experiments were conducted in essentially deep water. For deep water, the Wehausen period is given by the simple formula

$$T\sqrt{g/L} = 4\pi F \tag{1}$$

in which T is the period, g is the acceleration due to gravity, L is the model length, and F is the length-based Froude number.

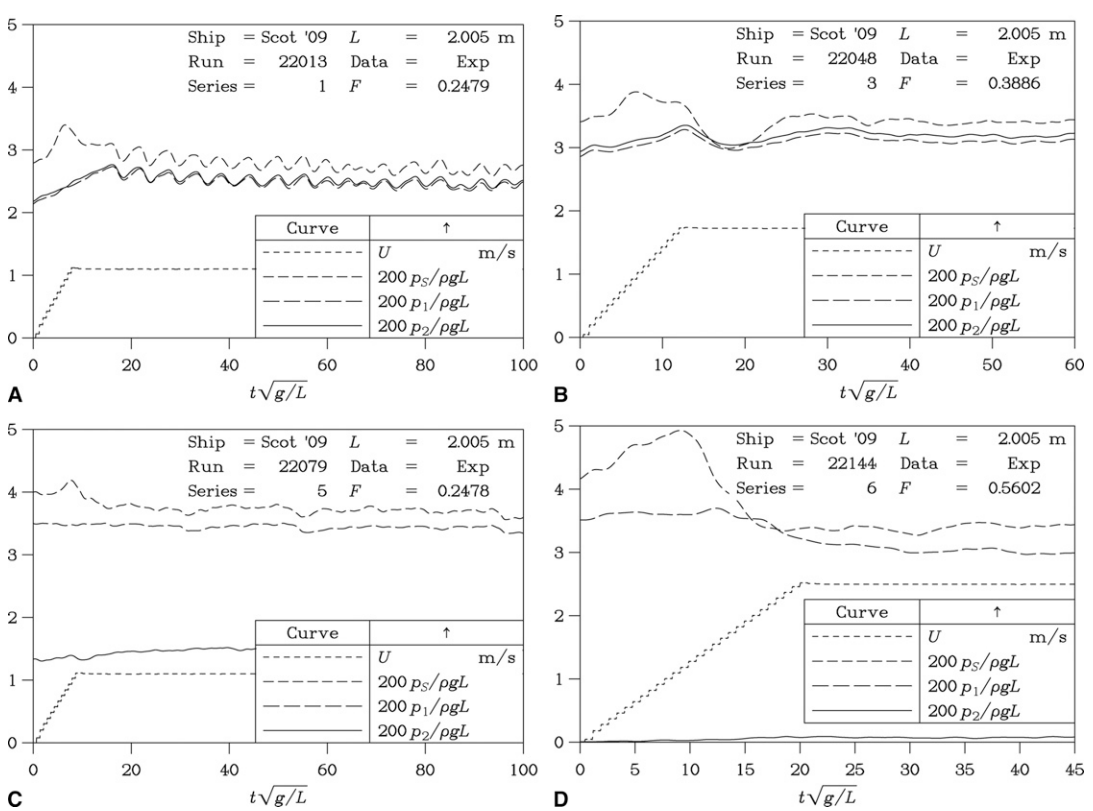

Fig. 3 Temporal pressure traces. *a* Series 1, $F = 0.2479$. *b* Series 3, $F = 0.3886$. *c* Series 5, $F = 0.2478$. *d* Series 6, $F = 0.5602$

The Wehausen formula gives a dimensionless period of $T\sqrt{g/L} = 4\pi \times 0.2479 = 3.115$, whereas the curves possess a dimensionless period of approximately 5.0. So, the two phenomena are unrelated.

For the purpose of the analysis, the curves were averaged over the last 60% of the run before the carriage was arrested. It may be noted that the two subcushions have essentially identical pressures as expected, while the aft seal is at a higher pressure, which is normal.

Figure 3*b* is a plot taken from another run, from series 3, in the towing tank. In this case, the high-frequency oscillations of Fig. 3*a* do not occur. However, there is still a certain level of unsteadiness in the data.

Figure 3*c* represents an example of the two-subcushion configuration, namely series 5. The substantial and intentional difference between the pressures in the two subcushions is clear. Again, the stern seal pressure is higher than the aft-subcushion pressure.

Figure 3*d* is an example from series 6. The essentially zero pressure in the forward subcushion p_2 is seen. The slight unsteadiness in the pressure in the stern-lobe seal p_S and in the pressure in the aft subcushion p_1 is also noted.

5.3. Froude-number-dependent subcushions

The time averaged subcushion pressures are plotted in the five parts of Fig. 4, these corresponding to the test series listed in Table 4.

Thus, the stern seal pressure p_S, the aft-subcushion pressure p_1 and the forward-subcushion pressure p_2 are plotted as a function of the Froude number F in Fig. 4*a* for series 1. It may be noted that the two subcushions have essentially the same pressure (as expected for the single-large-cushion case). On the whole, the aft-seal pressure is higher than this cushion pressure. However, it is curious that at some speeds the aft-seal pressure is not higher. Despite this, the model in such cases appeared to operate properly, supported by its air cushion.

Ideally, it would have been desirable to have a precisely set fixed cushion pressure over the entire Froude-number range, thus

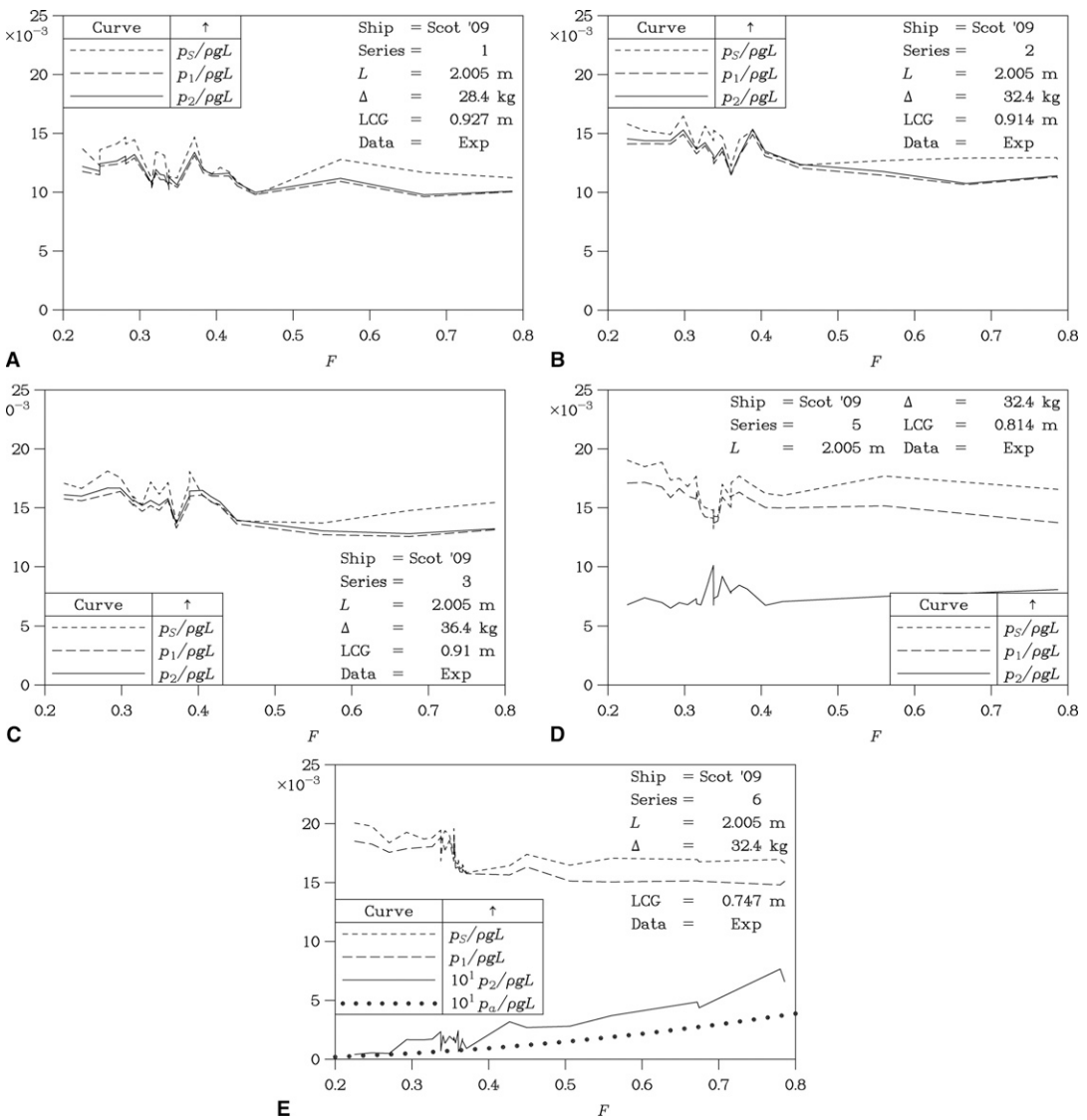

Fig. 4 Subcushion pressures. *a* Series 1. *b* Series 2. *c* Series 3. *d* Series 5. *e* Series 6

making the subsequent plots a little more meaningful. This does not seem to be possible without a sophisticated cushion-control system. Nevertheless, the theory for the resistance was applied using the measured cushion pressures, so that a consistent comparison of theory and experiment was effected.

Similarly, Fig. 4*b* for series 2 and Fig. 4*c* for series 3 are applied to the single-cushion case, but for higher displacements of the model.

Figure 4*d* applies to series 5 for the two-subcushion case. One may discern that the two subcushions possess substantially different pressures and that the stern seal is at the highest pressure.

The effect of small variations in the inner seal vertical position can be seen in Fig. 4*d* at a Froude number of 0.34. A series of tests was carried out at this speed, in which small variations were deliberately made in the lift-fan speeds and the inner-seal position. These variations in turn modified the level of leakage of air between the aft and forward subcushions, thus changing the pressure differential.

Figure 4*e*, for series 6, is for the single-short-cushion case. The forward subcushion is ideally zero in this case, because the bow-finger seal was removed. Nevertheless, we see that there is still some pressure p_2 in that region of the model. Note that a factor of 10 has been applied to the vertical scale to clarify this point. This pressure is compared with the aerodynamic ram pressure $p_a = \frac{1}{2}\rho_a U^2$, where ρ_a is the density of the air. There is sufficient difference between these two pressures to suggest that the pressure in the region of the forward-subcushion cannot be explained as being generated by the air ram pressure alone.

6. Resistance of model surface-effect ship

6.1. Resistance components

We now turn to Fig. 5, consisting of five parts, corresponding to the principal test series listed in Table 4. Figure 5*a* is a plot of the

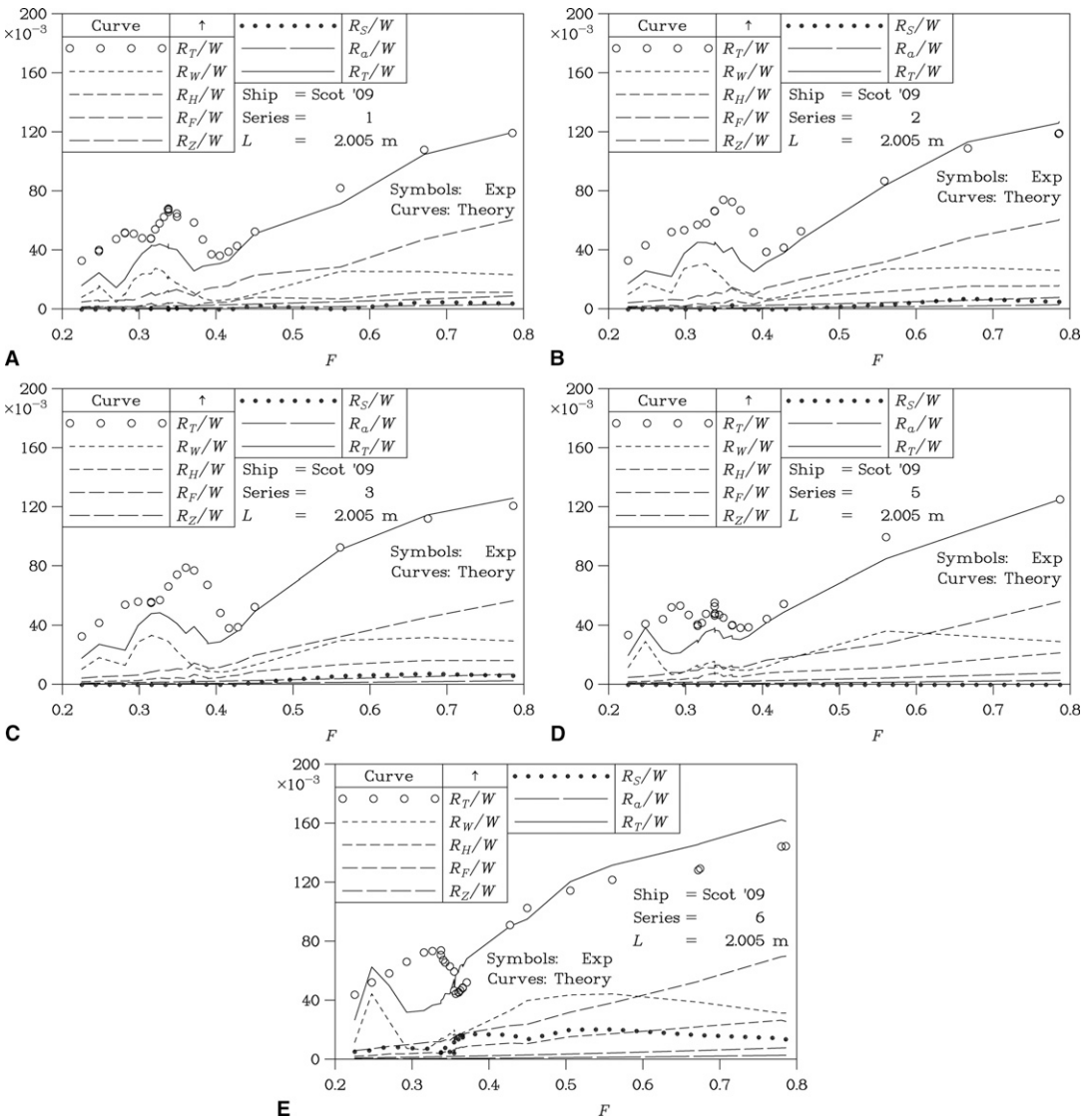

Fig. 5 Resistance components. *a* Series 1. *b* Series 2. *c* Series 3. *d* Series 5. *e* Series 6

Table 5 Resistance components

Symbol	Meaning
R_F	Frictional
R_H	Hydrostatic
R_S	Bow seal
R_T	Total
R_W	Wave
R_Z	Stern seal
R_a	Air

resistance components listed in Table 5. The graph applies to series 1.

The six theoretical resistance components are plotted, together with the total theoretical resistance. The latter was evaluated through the formula:

$$R_T = R_W + R_H + f_F R_F + R_Z + R_S + R_a \tag{2}$$

The components have been made dimensionless using the vessel weight W. These are now referred to as the specific-resistance components. The graph shows that the wave resistance R_W and the frictional resistance R_F are the principal contributors to the resistance of the model. The frictional resistance was estimated using the 1957 International Towing Tank Committee (ITTC) formula, described by Lewis (1988, Section 3.5). The transom hydrostatic resistance R_H is also important—at least at high values of the Froude number F.

The drag of the stern-lobe seal R_Z is modeled on the basis of its frictional resistance, estimated from the geometry and the assumed contact area with the water. This drag component is seen to be small. The drag of the bow-finger seal R_S is modeled according to the planing theory developed by Doctors and McKesson (2006). It is also relatively small.

The present outcome of a low value for the bow-seal drag contrasts with the calculations of Doctors and McKesson (2006), where the seal drag could be substantial, particularly at near-hump speeds. The explanation is that the current SES model was specifically designed for minimal seal water contact in the design condition. This corresponds to a nominal draft T of 0.080 m, as noted in Table 2.

The aerodynamic drag R_a is also a small contributor.

Finally, the theoretical total resistance R_T is a simple sum, assuming a frictional form factor f_F of 1.150. This is similar to the value of 1.180 used by Doctors and McKesson (2006). This value of the frictional form factor was determined in order to produce agreement between theory and experiment for the total resistance at high speeds. It is partly justified on the basis that similar values of the frictional form factor have been successful in the past.

On the whole, there is excellent agreement with the experimental data points, at a Froude number greater than 0.40. At lower speeds, it would appear that the underprediction of the theory may be due to our simplistic drag model for the rear-lobe seal.

Similar comments can be made about Fig. 5*b* for series 2, Fig. 5*c* for series 3, Fig. 5*d* for series 5, and Fig. 5*e* for series 6.

The effect of varying pressure differential between the subcushions can be seen in Fig. 5*d* (and also in Fig. 6*c* and Fig. 6*d*) in the series of points at a Froude number of 0.34. As mentioned previously in section 5.3, these points were obtained by deliberately making subtle variations in the ratio of pressures between the forward and aft subcushions, thus affecting the resistance.

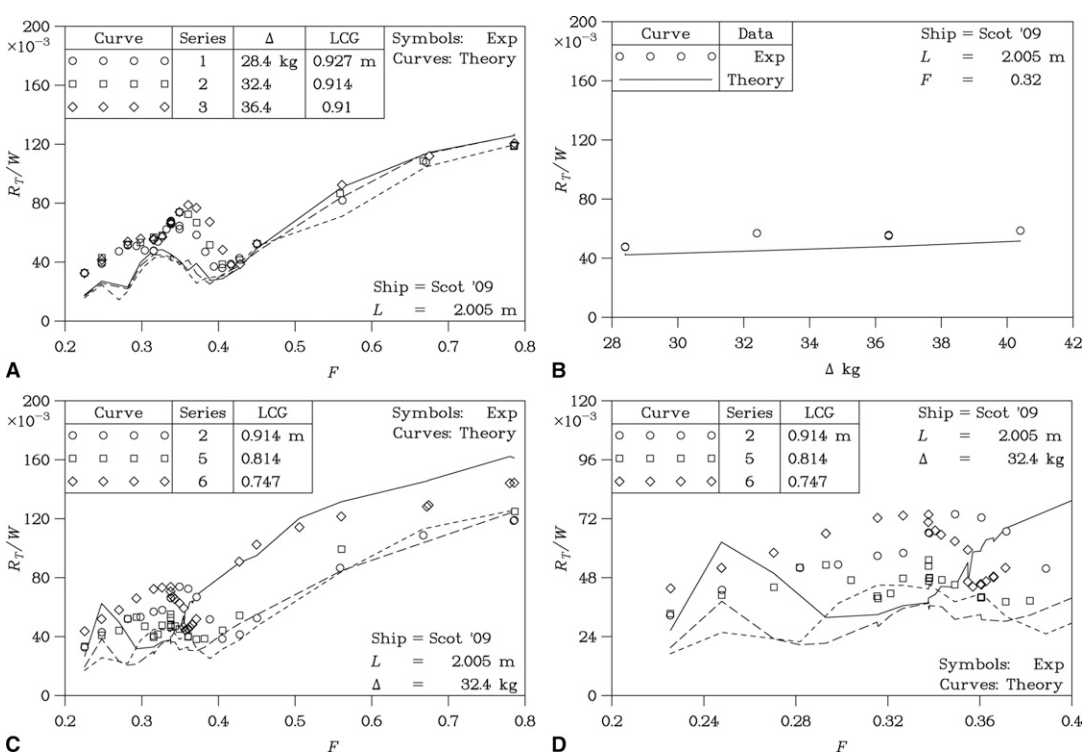

Fig. 6 Variations in loading. *a* Function of the Froude number. *b* Function of the displacement. *c* Function of the compartmentation. *d* Function of the compartmentation (low speed)

6.2. Variation in loading of model

We complete the presentation of our analysis by replotting the total resistance R_T from the various parts of Fig. 5.

Thus, Fig. 6*a* is a comparison of the results for total resistance from series 1, series 2, and series 3. This is our approximation to a *test of linearity* of the hydrodynamic theory. There are a number of issues complicating such a test. The principal issue is that the frictional resistance of the sidehulls will mask much of the interesting hydrodynamic-wave effects. Nevertheless, the essential point is that the theory is evaluated for the same conditions of the experiment. Hence, the comparison will be valid.

The reader can identify the loading configuration (the particular series) by noting its number and referring to Table 4. The corresponding value of the LCG can be used as further confirmation.

A vital warning with respect to interpreting the three theoretical curves and the three sets of data points, corresponding to the three different displacements, is that we are plotting the *specific resistance,* not the resistance itself. Hence, the marked and expected increase in resistance with the displacement is not apparent to a large extent. Despite this, it is gratifying to note that the theory can effectively distinguish between the curves of specific resistance when the Froude number exceeds 0.40. That is, the theory correctly orders the three sets of results.

The cross plot of specific total resistance, at a Froude number of 0.32, as a function of the model displacement, appears in Fig. 6*b*. The slight increase in specific resistance with displacement in the experiment is confirmed by the theory.

Finally, Fig. 6*c* is a plot illuminating the effectiveness of cushion compartmentation. We have plotted the data for the intermediate displacement of 32.4 kg. Thus, series 2 for the single-cushion configuration, series 5 for the two-subcushion configuration, and series 6 for the single-short-cushion configuration are plotted. The last case is also effectively a two-subcushion configuration, but with near-zero pressure in the forward subcushion.

We can again report that, for a Froude number exceeding 0.40, the theory provides a good correlation with the experiments and can correctly order the three sets of results. Indeed, the minor crossover effect for the first two theoretical curves is confirmed by the data from the experiments.

Because the data is somewhat confusing at the low end of the speed range, we have replotted it on an expanded scale in Fig. 6*d*, in order to make it clearer.

7. Concluding comments

- The tests successfully demonstrated that the partitioning of the cushion has the desired effect of dramatically reducing the main hump in the resistance curve. An examination of Fig. 6*c* demonstrates how vastly differing resistance values can be obtained by changing the subcushion configuration. For example, at a Froude number near 0.32, series 5, representing the standard two-subcushion case, possesses at least 40% less total resistance than the single-cushion configuration.
- Shortening the cushion moves the hump to lower speed, but requires a larger movement of LCG, and gives higher resistance at all speeds than the partitioned case. At higher speeds, beyond the main hump, the single cushion gives the lowest resistance in all cases.
- For a Froude number exceeding 0.40, the traditional linearized hydrodynamic theory for the wave resistance, together with estimates for the other resistance components, provides an excellent prediction of the total resistance.
- For a Froude number less than 0.40, the theory provides a qualitative indication of the behavior, but is less effective in predicting total resistance quantitatively. This is in contrast to the outcome from previous studies, such as that of Doctors and McKesson (2006). It is interesting to note that the locations (as well as the magnitudes of the humps and hollows) are displaced relative to the experiment results. One inference that can reasonably be drawn from this observation is that the model currently employed is not accounting adequately for all aspects of the extremely complex wavemaking behavior of this type of vessel in this speed regime. In particular, the model currently employed for the stern seal only accounts for frictional resistance; it is possible that this should be extended to investigate the impact of the stern seal on the wavemaking of the SES.
- Regarding future work, we suggest a close study, through experiments, of the resistance behavior of the bow seal and the stern seal on an individual basis.
- Useful future theoretical work would include a careful analysis of the resistance of the stern-lobe seal. Such an analysis could be based on modeling this seal as a membrane with a differential pressure across its thickness. The pressure differential would have to be determined as part of the solution. Thus, the proper dynamic shape of the seal would be found. Such a theory would be analogous to planing theory and will yield an additional component of drag due to the spray.

Acknowledgments

We would like to thank the University of Strathclyde for providing the Sir David Anderson Bequest Award, which supported travel and maintenance costs associated with this project, as well as the Department of Naval Architecture and Marine Engineering for additional funding.

We would also like to express our appreciation to Mr. Charles Keay, Laboratory Coordinator, who supervised the construction of the model SES and the associated specialized equipment. Additionally, he oversaw the operation of the towing tank.

Finally, we also respectfully acknowledge the infrastructure support provided by both the University of Strathclyde and The University of New South Wales (UNSW).

References

Barratt, M. J. 1965 The wave drag of a hovercraft, *Journal of Fluid Mechanics,* **22,** Part 1, 39–47.

Beveridge, P. 2009 *Design, Build, Test and Analysis of a Model SES with Partitioned Cushion Arrangement,* University of Strathclyde, Department of Naval Architecture and Marine Engineering, Bachelor's thesis, 76 pages May.

Day, A. H., Clelland, D., and Doctors, L. J. 2009 Unsteady finite-depth effects during resistance tests in a towing tank, *Journal of Marine Science and Technology,* **14,** 3, 387–397.

Day, A. H., and Doctors, L. J. 1997 Resistance optimization of displacement vessels on the basis of principal parameters, *Journal of Ship Research*, **41,** 4, 249–259.

Doctors, L. J. 1993 On the use of pressure distributions to model the hydrodynamics of air-cushion vehicles and surface-effect ships, *Naval Engineers Journal,* **105,** 2, 69–89.

Doctors, L. J. 1997 Optimal pressure distributions for river-based air-cushion vehicles, *Ship Technology Research: Schiffstechnik,* **44,** 1, 32–36.

Doctors, L. J. 2007 A numerical study of the resistance of transom-stern monohulls, *Ship Technology Research: Schiffstechnik,* **54,** 3, 134–144.

Doctors, L. J., and Day, A. H. 1995 Hydrodynamically optimal hull forms for river ferries, *Proceedings,* International Symposium on High-Speed Vessels for Transport and Defence, Royal Institution of Naval Architects, London, England, November, 5.1–5.15.

Doctors, L. J., and Day, A. H. 1997 Resistance prediction for transom-stern vessels, *Proceedings,* Fourth International Conference on Fast Sea Transportation (FAST '97), Sydney, Australia, July, vol. 2, 743–750.

Doctors, L. J., Macfarlane, G. J., and Young, R. 2007 A study of transom-stern ventilation, *International Shipbuilding Progress*, **54,** 2, 3, 145–163.

Doctors, L. J., and McKesson, C. B. 2006 The resistance components of a surface-effect ship, *Proceedings,* 26th Symposium on Naval Hydrodynamics, Rome, Italy, 14 pages, September.

Doctors, L. J., Tregde, V., Jiang, C., and McKesson, C. B. 2005 Optimization of a split-cushion surface-effect ship, *Proceedings Eighth International Conference on Fast Sea Transportation (FAST '05)*, Saint Petersburg, Russia, June, 8 pages.

Lewis, E. V. editor 1988 *Principles of Naval Architecture: Volume II. Resistance, Propulsion and Vibration,* Society of Naval Architects and Marine Engineers, Jersey City, NJ, 327 + vi pages.

Lin, W.-C., Webster, W. C., and Wehausen, J. V. 1963 *Ships of Minimum Total Resistance,* University of California, Institute of Engineering Research, Berkeley, CA, August, 47 + ii pages, Report NA-63-7.

Michell, J. H. 1898 The wave resistance of a ship, *Philosophical Magazine, London, Series 5,* **45,** 106–123.

Newman, J. N., and Poole, F. A. P. 1962 The wave resistance of a moving pressure distribution in a canal, *Schiffstechnik,* **9,** 45, 21–26.

Oving, A. J. 1985 Resistance prediction method for semi-planing catamarans with symmetrical demihulls, *Proceedings,* Maritime Research Institute Netherlands (MARIN), Wageningen, September, 79 + i pages.

Sretensky, L. N. 1936 On the wave-making resistance of a ship moving along in a canal, *Philosophical Magazine, Series 7, Supplement,* **22,** 150, 1005–1013.

Steen, S., and Adriaenssens, C. 2005 Experimental verification of the resistance of a split-cushion surface-effect ship, *Proceedings,* Eighth International Conference on Fast Sea Transportation (FAST '05), Saint Petersburg, Russia, June, 8 pages.

Tuck, E. O., and Lazauskas, L. 2001 *Free-Surface Pressure Distributions with Minimum Wave Resistance,* University of Adelaide, Department of Applied Mathematics, January, 19 pages.

Wehausen, J. V. 1964 Effect of the initial acceleration upon the wave resistance of ship models, *Journal of Ship Research*, **7,** 3, 38–50.